The Inhibitory Monoclonal Antibody M7-PB-E9 Stabilizes E_2 Conformational States of Na^+,K^+-ATPase†

Alan Abbott and William J. Ball, Jr.*

Department of Pharmacology and Cell Biophysics, University of Cincinnati, College of Medicine, Cincinnati, Ohio 45267-0575

Received May 21, 1992; Revised Manuscript Received September 2, 1992

ABSTRACT: Monoclonal antibody M7-PB-E9 binds the sheep kidney Na^+,K^+-ATPase α-subunit with high affinity (K_d = 3 nM) and inhibits enzyme turnover in competition with ATP, and, like ATP, in the presence of Mg^{2+}, it stimulates the rate of ouabain binding [Ball, W. J. (1984) *Biochemistry 23,* 2275–2281]. In this study, covalent attachment of fluorescein 5′-isothiocyanate (FITC) at (or near) the enzyme's ATP binding site did not alter the antibody's affinity for α nor did bound antibody alter the anisotropy of (r = 0.36) or the solvent accessibility of iodide to bound FITC. Further, in its E_1Na^+ conformation (4 mM NaCl), the enzyme's affinity for the ATP congener eosin was unaltered by the bound antibody (K_d = 9 nM). In contrast, partial E_2 conformations induced by KCl lowered eosin affinities (0.2 mM KCl, K_d = 28 nM; 0.4 mM, K_d = 86 nM), and M7-PB-E9 reduced these affinities further (K_d = 66 and 130 nM, respectively). By monitoring the fluorescence changes of the FITC-labeled enzyme, the antibody was found to assist several ligand-induced conformational transitions from E_1 (E_1Na^+ or E_1Tris) to E_2 (E_2K^+, E_2–P_iMg^{2+}, or E_2Mg^{2+}·ouabain) states, and inhibit the $E_2K^+ \rightarrow E_1Na^+$ transition. Antibody binding alone, however, did not appear to significantly alter enzyme conformation. The antibody therefore is not directed against the ATP site but binds to a region of α distinct from any ligand binding site and which plays an important role in the $E_1 \rightleftarrows E_2$ transitions.

Na^+,K^+-ATPase (EC 3.6.1.3) is the integral membrane protein which actively pumps Na^+ and K^+ across the plasma membrane against their electrochemical gradients using the energy of ATP hydrolysis. The enzyme is known to be composed of at least two subunits: the catalytic α-subunit (M_r ~112K) and the smaller, glycosylated β-subunit (M_r ~55K). The α-subunit binds all known physiological and pharmacological ligands and catalyzes all partial reactions associated with the active enzyme while the β-subunit appears essential for the integrity or expression of active enzyme in the cellular membrane (Geering, 1991).

Extensive investigation of the enzyme's reaction mechanism [reviewed by Glynn (1985)] has shown that Na^+ and K^+ are transported across the membrane through a series of conformational transitions between the E_1 and E_2 states of the enzyme with ion binding sites facing inside or outside the cell, respectively. This ion transport requires ATP hydrolysis and involves formation of a phosphoenzyme intermediate, E_1~P, that is formed by ATP in the presence of intracellular Na^+ and spontaneously changes to E_2–P with the transport of Na^+ to an extracellular low-affinity site. This exposes the high-affinity extracellular K^+ binding sites, and K^+ binding promotes the release of Na^+ and phosphate. The resultant $E_2(K^+)$ form is said to occlude K^+ because of its slow rate of release ($t_{0.5}$ > 1 s), but in the presence of ATP, the K^+ is transported to an intracellular low-affinity site, and the enzyme assumes an E_1ATP conformation which binds intracellular Na^+ with high affinity.

In order to understand the structural basis of this reaction mechanism (shown in Scheme I), several approaches have been used to identify amino acids which are essential for activity or contribute to ligand binding. For example, several different residues on the intracellular portion of α react with ATP analogues, and they may contribute to ATP binding [reviewed by Pedemonte and Kaplan (1990)] while carboxylate groups reacting with carbodiimides may be essential for cation binding (Karlish & Goldschleger, 1991). In addition, site-directed mutagenesis has been used to identify two amino acids critical to high-affinity ouabain binding (Price & Lingrel, 1988).

Scheme I

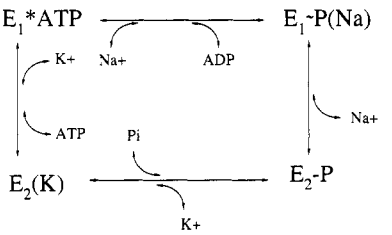

We have used an immunochemical approach to probe enzyme structure and function and have investigated the properties of several high-affinity antibodies that inhibit enzyme activity (Ball, 1984, 1986; Friedman & Ball, 1989). The inhibition by one of these antibodies, M7-PB-E9, was shown by Ball (1984) to be competitive with respect to ATP and decrease phosphoenzyme intermediate formation, but its effects on enzyme conformation or the partial reactions of catalytic turnover were not fully understood. For example, in addition to inhibiting the ATPase activity, it also enhanced ouabain binding in a manner that mimicked the effect of ATP, but these results did not distinguish between antibody-caused alterations in the $E_1 \leftrightarrow E_2$ enzyme conformational equilibrium or actual competition for the ATP binding site.

In the present study, antibody effects on enzyme conformation and ligand binding were monitored using the fluorescence changes undergone by the fluorescein 5′-isothiocyanate (FITC)[1]-labeled enzyme, and the ATP congener eosin was used in a fluorescence assay to investigate ATP binding.

† This work was supported by Research Grant HL-R01-32214 (W.J.B.) and Training Grant T32-HL-07382 from the National Institutes of Health and by an Ohio Affiliate Fellowship from the American Heart Association (A.A.).

* To whom correspondence should be addressed.

0006-2960/92/0431-11236$03.00/0

Our experiments show that antibody M7-PB-E9 has an effect on the $E_1 \leftrightarrow E_2$ conformational equilibrium and as a consequence alters not only ATP binding but also most of the other ligand bindings. The $E_1 \rightarrow E_2$ conformational transition, which is induced by several ligands, is assisted or stabilized by the antibody, and the reverse, the Na^+-dependent $E_2 \rightarrow E_1$ transition, is inhibited by the antibody. In addition, the extent of ligand-induced E_2 conformations was enhanced by bound antibody in the following order: E_2–$P_i Mg^{2+}$·OUAB > E_2–$P_i Mg^{2+}$ > $E_2 K^+$. The fact that ligands binding to both intra- and extracellular sites on the enzyme were affected suggests that the amino acids comprising the antibody's epitope play a pivotal role in enzyme functioning.

MATERIALS AND METHODS

Na^+,K^+-ATPase Isolation and Characterization. Na^+,K^+-ATPase was purified from the outer medulla of frozen lamb kidney according to the method of Lane et al. (1979) and stored at 4 °C until further use. The initial activity of the enzyme as determined using a spectrophotometric-linked enzyme assay was 1100 μmol of ATP hydrolyzed (mg of protein)$^{-1}$ h^{-1}. This preparation consists of lipid–protein vesicles with predominantly two protein bands corresponding to the molecular weights of the α- (110K) and β-subunits (55K) in evidence when it is resolved by SDS–PAGE.

FITC Labeling of the Na^+,K^+-ATPase. The Na^+,K^+-ATPase was diluted to a concentration of 1 mg/mL in 100 mM Tris-HCl, pH 9.1. Labeling with 10 μM FITC was accomplished by adding 1:100 (v/v) of 1 mM FITC freshly dissolved in dimethylformamide (DMF) in the dark for 30 min at 23 °C. Labeled enzyme (0.5 mL) was separated from unreacted probe by centrifugation of the sample (100*g*) twice through 3-mL columns of G-50 Sephadex. The labeling stoichiometry was quantitated by releasing a fluorescein-labeled peptide from a known amount of holoenzyme by tryptic digestion (one-tenth weight fraction of trypsin, 1 h, 37 °C, pH 8.0) and quantitating the peptide-bound fluorescein fluorescence relative to a free probe standard. Throughout this study, the labeling stoichiometry was 2.3–2.6 nmol of FITC/mg of protein.

Antibody Binding. The antibody affinity for the Na^+,K^+-ATPase and FITC–Na^+,K^+-ATPase antigens was measured by ELISA assay, as described earlier (Ball, 1984). Antigens were adsorbed to wells of 96-well microtiter plates (Costar 96 well plate 3596) for 1 h with 100 μL/well at 0.2 mg/mL. The solutions were then removed, and plate wells were washed with buffer A (10 mM Tris, 140 mM NaCl, 5 mg/mL BSA, and 0.02% NaN_3) and exposed to various concentrations of antibody, in buffer A for 1 h. The antibody solution was then removed, the plates were washed, and bound antibody was detected using a β-galactosidase–sheep anti-mouse IgG F(ab)'2 conjugate and *o*-nitrophenyl β-galactoside (ONPG) as substrate.

Steady-State Fluorescence Measurements. Steady-state fluorescence and light-scattering intensities were measured using an SLM/AMINCO (Urbana, IL) SPF-500 spectrofluorometer. FITC-labeled protein (5–20 μg) was suspended in 2.5 mL of 0.05 M Tris-HCl and 1 mM EGTA, pH 7.4, under continuous stirring at 25 °C. Samples were excited at 495 nm (4-nm band-pass width), and the emission was recorded at 520 nm (10-nm band-pass width). Ligand binding was measured by monitoring changes in FITC fluorescence intensity upon their titration directly into the cuvette from stock solutions (e.g., 2 M NaCl, 2 M KCl, 1 M Tris–PO_4, 1 M $MgCl_2$, and 1 mM ouabain). The extent of binding was calculated as the percent change in fluorescence intensity relative to the total fluorescence change observed under saturating ligand conditions. All measurements were corrected for dilution. In initial experiments, to ensure complete antibody binding, the FITC–enzyme was preincubated in a small volume (50 μL) with excess (10–30 μg) antibody for 20 min, before dilution of the sample into the 2.5-mL assay solution. This proved unnecessary and in later experiments antibody was added directly to the diluted enzyme samples in the fluorescence cuvettes. Steady-state anisotropy values (*r*) were calculated from polarization values as previously described (Abbott et al., 1991).

Eosin B (referred to as eosin) fluorescence was measured upon its binding to native holoenzyme. Samples were excited at 520 nm (4-nm band-pass width), and emission was recorded at 540 nm (10-nm band-pass width). The fluorescence increase upon titration of Na^+,K^+-ATPase (20 μg/mL, or about 100 nM in 0.05 M Tris-HCl/2 mM EGTA, pH 7.5, buffer) with increasing eosin (0–390 nM) was measured relative to that of eosin alone. Enzyme samples (20 μg/mL) with antibody M7-PB-E9 present were preincubated 30 min with 35 μg/mL antibody. The quantum yield increase of 59 nM eosin upon binding to saturating enzyme (200 μg/mL, about 1 μM) was 11.1-fold. This is significantly higher than that reported earlier by Skou and Esmann (1981) and may result from our using eosin B (the xanthone ring modified with two bromine atoms and two nitrate groups) rather than eosin Y (four bromines) as in their study. Total eosin fluorescence in the presence of enzyme (F_{b+f}) can be expressed as a function of eosin fluorescence in the absence of enzyme (F_0) and its quantum yield increase upon binding:

$$F_{b+f} = F_0 f_b(11.1) + F_0 f_f \quad (1)$$

where f_b and f_f are the fractions bound and free, respectively. Rearranging eq 1 and inserting $f_f = 1 - f_b$, the fraction of eosin bound was calculated for each titration point:

$$f_b = (F_{b+f} - F_0)/F_0 10.1 \quad (2)$$

Since the total molar amounts of eosin and enzyme present were known, the concentrations of enzyme bound and free or eosin could then be calculated.

Use of Light Scattering To Measure the Kinetics of Antibody Binding to the Unlabeled Enzyme Preparation. Raleigh light scattering was measured by setting both the excitation and emission wavelengths to 500 nm. This wavelength was selected because it is large relative to the scattering particle diameter and there was negligible absorbance or fluorescence of the sample. The time course of antibody binding was measured by adding a 3-fold excess of antibody (27.5 μg/mL final concentration, dead time = 1 s) to 9.2 μg/mL Na^+,K^+-ATPase and monitoring the increase in the light-scattering intensity (I_s). Binding was reported as the relative increase in proteolipid (or scattering particle) molecular weight according to Nelsestuen and Lim (1977):

$$M_2/M_1 = \sqrt{I_{s2}/I_{s1}} \quad (3)$$

where subscripts 1 and 2 refer to before and after antibody binding, respectively. The time course for $\sqrt{I_{s2}/I_{s1}}$ to reach a maximum is shown in Figure 6.

[1] Abbreviations: DMF, dimethylformamide; ELISA, enzyme-linked immunosorbent assay; FITC, fluorescein 5'-isothiocyanate; mAb, monoclonal antibody; OUAB, ouabain; PAGE, polyacrylamide gel electrophoresis; SDS, sodium dodecyl sulfate.

It must be noted that the bound antibody will affect the scattering particle's diameter and its refractive index, and as a result the scattering intensity change will depend on the particle scattering factor, $P(\theta)$, and the refractive index increment ($\partial n/\partial C$) as well as the molecular mass according to the equation of Doty and Edsall (1951):

$$I_{s2}/I_{s1} = (M_2/M_1)^2[(\partial n_2/\partial C_2)/(\partial n_1/\partial C_1)]^2 P(\theta)_2/P(\theta)_1 \quad (4)$$

where subscripts 1 and 2 still refer to before and after antibody binding, respectively, and n is the refractive index while C is the weight concentration (Nelsestuen & Lim, 1977). Equation 3 results from setting both $[(\partial n_2/\partial C_2)/(\partial n_1/\partial C_1)]^2$ and $P(\theta)_2/P(\theta)_1$ equal to 1, and this is justified according to our estimates of their values. For example, if the antibody (MW = 150K) were to bind to all the enzyme molecules (MW = 150K) present, the overall protein weight in each particle would double, and because the enzyme and lipid are present in approximately equal weight amounts in our preparation (Lane et al., 1979), the proteolipid vesicle molecular weight would be 1.5 times its original value. Under these conditions, $(M_2/M_1)^2 = 2.25$, and the refractive index increment terms, $\partial n_2/\partial C_2$ and $\partial n_1/\partial C_1$, can be estimated by adding the products of the refractive index increment and fractional contribution (by weight) for both lipid and protein. In the current example, using the refractive index increments for lipid ($\partial n/\partial C = 0.172$) and protein ($\partial n/\partial C = 0.192$) measured by Nelsestuen and Lim (1979), the calculated refractive index increment ratio, $[(\partial n_2/\partial C_2)/(\partial n_1/\partial C_1)]^2$, is 1.033. The scattering factor $P(\theta)$, on the other hand, is based on the vesicle diameter [200 nm; our unpublished observations and Van Winkle et al. (1976)] and can be calculated using the analytical expression for a spherical particle (Doty & Edsall, 1951). For an estimated maximum increase in vesicle diameter, from 200 to 216 nm—assuming antibody is packed on the membrane surface with its long axis of 80 Å (Silverton et al., 1977) perpendicular to the membrane surface—$P(\theta)_2/P(\theta)_1 = 0.89$. Therefore, compared to the increase of $(M_2/M_1)^2$ upon antibody binding ($1 \rightarrow 2.25$ in the above example), $[(\partial n_2/\partial C_2)/(\partial n_1/\partial C_1)]^2$ would maximally increase 3.3% ($1 \rightarrow 1.033$) and $P(\theta)_2/P(\theta)_1$ decrease 11% ($1 \rightarrow 0.89$). In fact, the actual observed increase in I_{s2}/I_{s1} was $1.0 \rightarrow 1.16$, and the contribution due to any changes in the refractive index increment and the scatter factor terms should be substantially less than 10% of the scattering intensity increase, and they were assumed to be unchanged.

The possibility that the light-scattering intensity change which occurred upon antibody addition was due to vesicle aggregation was discounted by direct electron microscopic visualization of the negatively stained vesicles. The average diameter of our vesicles was 185 ± 80 nM ($n = 24$). There was considerable size heterogeneity but no apparent vesicle aggregation in either the presence or the absence of M7-BP-E9. In addition, antibodies 9-A5 and M10-P5-C11 (Friedman and & Ball, 1989) caused similar light-scattering intensity increases when they bound the enzyme preparation.

Analysis of Equilibrium and Kinetic Binding Data. For ligand binding kinetics, the data were analyzed using a pseudo-first-order or single-exponential decay model [see Ball (1984)] for the fractional loss of unbound ligand sites. For ouabain binding, the data were fit to eq 5 using nonlinear least-squares curve fitting:

$$f_{\text{unbound}} = \exp(-kt) \quad (5)$$

while the kinetics of antibody binding were measured by monitoring both light-scattering and FITC fluorescence intensity changes (see Figure 6), and they were compared qualitatively in secondary plots of log f_{unbound} vs time. Equilibrium ligand binding was presented as the fraction of bound sites versus ligand concentration for a single binding site model

$$f_b = [L]/(K_d + [L]) \quad (6)$$

or for a cooperative binding sites model (n = Hill coefficient)

$$f_b = [L]^n/(K'_d + [L]^n) \quad (7)$$

or for a two noninteracting binding sites model (where α = fraction of total sites contributing to size 1)

$$f_b = \alpha[L]/(K_{d1} + [L]) + (1 - \alpha)[L]/(K_{d2} + [L]) \quad (8)$$

Values for K_d, K'_d, K_{d1}, K_{d2}, n, or α were found by the best nonlinear least-squares fit of the experimentally determined f_b and [L] values to the above equations. Cooperative binding was found for Na^+ and K^+ binding interactions while phosphate binding and eosin binding were fit by a single-site binding model. A model for two independent sites (eq 8) was necessary to describe Mg^{2+} binding to the E_2K^+ enzyme conformation.

Iodide Quenching of FITC–Na^+,K^+-ATPase. Iodide was used as a collisional quencher of the FITC-labeled enzyme. FITC fluorescence decreases were measured over a 0–100 mM choline iodide concentration since above this concentration enzymatic activity was observed to decrease. The choline salt of iodide was used because choline was found not to alter the enzyme conformation or Na^+ or K^+ effects. All titrations were performed in triplicate and plotted using the Stern–Volmer equation:

$$F_0/F = 1 + K_q[Q] \quad (9)$$

where F_0 and F are the fluorescence intensity in the absence of quencher and presence of quencher [Q], respectively. K_q is the dynamic Stern–Volmer quenching constant. The quenching constant was taken from the slope of the line of F_0/F versus [Q] as calculated by the linear least-squares best fit of the data. In all cases, the correlation coefficient for the fit of the data to a straight line was ≥0.997.

Other Procedures and Materials. Na^+,K^+-ATPase activity was measured spectrophotometrically in an ATP-regenerating, coupled enzyme assay (Schwartz et al., 1969). The protein concentration was determined by the Lowry procedure (Lowry et al., 1951). Antibodies conjugated to β-galactosidase and horseradish peroxidase were from Gibco–BRL (Gaithersburg, MD) and Calbiochem (San Diego, CA), respectively, and electrophoretic supplies and reagents were from Bio-Rad (Richmond, CA).

RESULTS

Previously the monoclonal antibody M7-PB-E9 was reported to have an "ATP-like" effect on Na^+,K^+-ATPase function (Ball, 1984). For example, it increased the rate of ouabain binding to the enzyme in the presence of Mg^{2+}, and its inhibition of the Na^+,K^+-dependent ATPase activity was competitive with respect to ATP. While it appeared that M7-PB-E9 could be acting at the ATP binding site, the mechanism of its effects remained somewhat obscure. The present work investigates this issue.

Antibody Effects on Enzymatic Activity. First we verified the inhibitory effect of M7-PB-E9 on the Na^+,K^+-dependent ATPase activity. The enzyme was preincubated 30 min with increasing antibody concentrations in the absence of any ligands. Aliquots were then diluted 10-fold into the assay solution, and the activity was determined. Despite this dilution

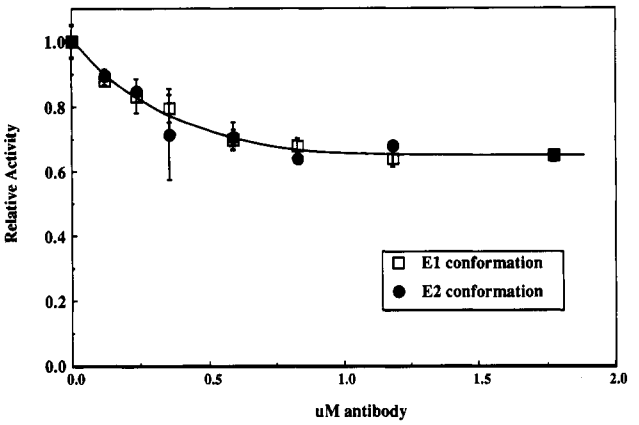

FIGURE 1: Inhibition of Na^+,K^+-ATPase activity by mAb M7-PB-E9. The enzyme (0.1 mg/mL, 0.7 μM) was preincubated 30 min with 2 μM antibody in the presence of 20 mM NaCl (open squares, E_1 conformation) or 20 mM KCl + 10 mM $MgCl_2$ (closed circles, E_2 conformation). The activity was then measured for 1 μg of enzyme diluted to 0.7 μg/mL into the ATPase assay solution containing 0.5 mM ATP. The activity curves are expressed as a percentage of the maximum activity in the absence of antibody.

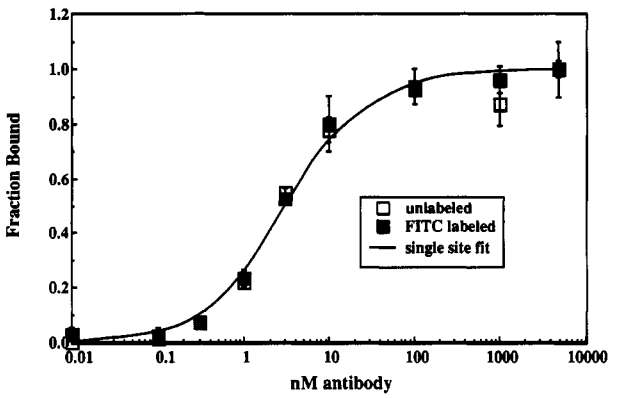

FIGURE 2: Affinity of mAb M7-PB-E9 for surface-adsorbed Na^+,K^+-ATPase and for FITC-labeled Na^+,K^+-ATPase. Plate-adsorbed, unlabeled (open squares) and labeled (closed squares) enzyme (0.5 mg/mL, 100 μL per well) was incubated with varying antibody concentrations (0–4800 nM), and binding was detected using a β-galactosidase-conjugated second-antibody colorometric assay (described under Materials and Methods). The data were fit to a single-site binding equation with half-maximal binding at 2.9 nM antibody.

step, the enzyme and antibody concentrations were still above the ELISA assay determined titer values for antibody binding to the enzyme (2.9 nM; see Figure 2), and linear activity rates during the course of the assays were observed. In the presence of high ATP (5 mM) concentrations, no inhibition was observed (data not shown), but under limiting ATP concentrations (0.5 mM), the activity was inhibited to a maximum of about 35% (see Figure 1). This was achieved with a roughly 1:1 enzyme:antibody stoichiometry. These results were in excellent agreement with those reported previously (Ball, 1984). In addition, the enzyme–antibody preincubations were also carried out in several different ligand conditions (Na^+, K^+, K^+Mg^{2+}, and $Mg^{2+}+P_i$) in order to determine if this would alter the stability of the enzyme–antibody complex. The antibody inhibition curves were unaffected by preincubation with these ligands, and Figure 1 shows the curves obtained following Na^+ and K^+Mg^{2+} preincubations.

Characterization of FITC and Antibody Interactions. When covalently bound to the enzyme, FITC is likely to be at or near the ATP binding site because it blocks ATP binding and labels lysine-501 of α (Farley et al., 1984) which resides within the consensus sequence for the enzyme's nucleotide binding domain (Taylor & Green, 1989). The ability of bound FITC to alter M7-PB-E9 binding was investigated using an ELISA procedure. Figure 2 shows the binding curve for the antibody titration of unlabeled and FITC-labeled enzyme. In both cases, the binding curve fit a single-site model (solid line, Figure 2) with identical affinities of 2.9 nM for half-maximum binding. Therefore, the fluorescein moiety did not affect the antibody affinity for the enzyme.

The fluorescence polarization of enzyme-bound FITC was then measured to determine possible effects of bound antibody on the rotational flexibility or degree of reorientation of fluorescein during its fluorescence lifetime (3.6 ns; Abbott et al., 1991). The anisotropy of the enzyme-bound probe was $r = 0.36$ when measured in Tris buffer, and it was unaltered by transitions to the E_1Na^+-, E_2K^+-, or E_2–P_iMg^{2+}-induced enzyme conformations. The addition of saturating antibody caused no changes in the anisotropy value (data not shown). M7-PB-E9 did not alter the nanosecond motional properties of enzyme-bound FITC.

Effect of Antibody on I^- Solvent Access to FITC. Despite its lack of effect on the probe's r value, if the antibody were to bind near the FITC labeling site(s) on α, it still might sterically reduce the diffusional access of solvent to the site. Solvent accessibility to bound FITC was therefore determined by measuring the quenching of FITC–Na^+,K^+-ATPase fluorescence upon addition of the collisonal quencher choline iodide. Linear Stern–Volmer plots were obtained, and the quenching constants (K_q) derived are a relative measure of I^- accessibility. In agreement with our previous work (Abbott et al., 1991), and K_q values for the Na^+- and K^+-induced conformations were 3.4 and 1.8 M^{-1}, respectively, and M7-PB-E9 had a negligible effect on both quenching constants (data not shown).

Antibody Effects on ATP Binding. The effect of mAb M7-PB-E9 on the affinity of the unlabeled enzyme for ATP was then indirectly measured using the ATP analog eosin (Skou & Esmann, 1981). Upon binding to the enzyme, the quantum yield of eosin was observed to increase 11.1-fold, and the resulting fluorescence increase was completely reversed by the addition of ATP (data not shown). Since ATP preferentially binds the E_1 conformation, the initial titration was performed in 4 mM Na^+. Figure 3 shows that M7-PB-E9 had no effect on the eosin titration curve with the enzyme in the E_1Na^+ conformation (see open and filled squares). In the presence of subsaturating levels of K^+, however, the affinity for eosin was reduced, and the antibody caused a significant further reduction in eosin affinity (Figure 3). Each of these curves was well fit by a single-site binding equation, and they revealed that KCl also reduced the maximum level of eosin binding and that the antibody reduced it further (Table I). Competition studies in which the bound eosin was displaced by increasing ATP concentrations gave an ATP inhibition constant (K_I) of 1 μM (data not shown), which is consistent with the previously published results of Moczydlowski and Fortes (1981). These data revealed that the eosin affinity and stoichiometry were unchanged by bound antibody with enzyme in the E_1Na^+ conformation but they are reduced with it partially in the E_2K^+ conformation. Unfortunately, eosin binding to the E_2K^+ enzyme in saturating K^+ concentrations could not be reliably detected.

Antibody Effects on Enzyme Conformation. The FITC-labeled enzyme was also used to define the effects of the antibody on ligand-induced conformational transitions. The "pseudo"-E_1 enzyme conformation induced by Tris buffer had the highest fluorescence E_1 (set at 100%), which was slightly

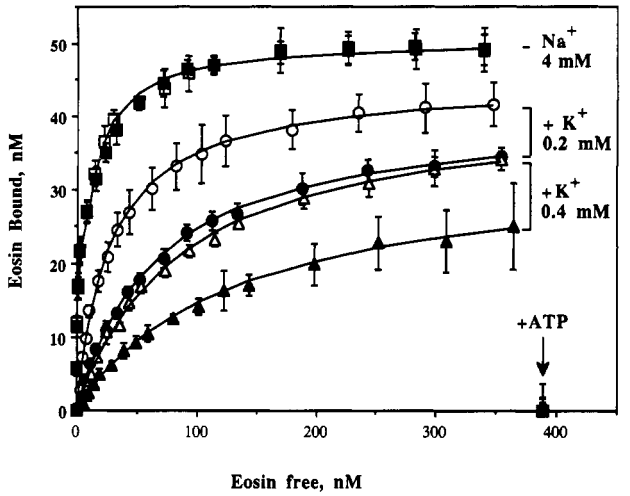

FIGURE 3: Effect of mAb M7-PB-E9 and K^+ on the Na^+,K^+-ATPase affinity for eosin. The enzyme (20 μg/mL) in 4 mM NaCl was titrated with 0–388 nM eosin, and binding was quantitated by the increase in eosin fluorescence (see Materials and Methods for details). Titrations in the presence (filled symbols) and absence (open symbols) of mAb M7-PB-E9 (31 μg/mL) were made in triplicate for Na^+-only conditions (squares) and in the presence of 0.2 mM (circles) and 0.4 mM (triangles) KCl. The lines show the curves generated by fitting the data to a single-site binding equation in which the K_d and maximum bound values were variable parameters (see Table I). The point on the horizontal axis at an eosin concentration of 388 mM shows that 0.9 mM ATP completely prevented eosin binding.

Table I: Effect of Ligand Conditions and M7-PB-E9 upon the Affinities of Eosin Binding to Na^+,K^+-ATPase[a]

ligand addition, [KCl] (mM)	eosin binding, K_d (nM)		max bound (nm)	
	-mAb	+mAb	-mAb	+mAb
0	8.6	9.0	50	50
0.2	28	66	41	41
0.4	86	130	42	33

[a] Na^+,K^+-ATPase in 0.05 M Tris, 4 mM NaCl, and 1 mM EGTA, pH 7.5, was titrated with eosin (0–400 nM). The K_d affinity values and maximum level bound for eosin in the presence (+mAb) and absence (-mAb) of antibody M7-PB-E9 were found by fitting the data to a single-site binding equation (Figure 3). The partial E_1Na^+/E_2K^+ conformations were induced with 0.2 and 0.4 mM additions of KCl.

reduced by Na^+ binding (E_1Na^+, 97%) and significantly reduced when the E_2 conformation was induced by K^+ (E_2K^+, 69%; $E_2K^+Mg^{2+}$, 79%), Mg^{2+}+P_i (E_2–P_iMg^{2+}, 68%), or ouabain (E_2Mg^{2+}·OUAB or $E_2P_iMg^{2+}$·OUAB, 48%). These fluorescence changes are similar to those reported by Hegyvary and Jorgensen (1981) and are consistent with the transition from the E_1 to the E_2–P_iMg^{2+}·OUAB conformation being the largest conformational rearrangement of the native enzyme because it shows the largest change in fluorescence. Fluorescence from nonspecifically bound probe was also present (Abbott et al., 1991), but since it is unaffected by ligand additions, it only contributed a modest constant background fluorescence.

Monoclonal antibody M7-PB-E9 was found to have little effect on enzyme conformation in the presence of saturating ligands. For example, the FITC fluorescence of the E_1Na^+ conformation (4 mM Na^+) was decreased only about 5% and 1% for the E_2K^+ form (1.8 mM K^+) upon antibody addition. In addition, the FITC fluorescences of the $E_2K^+Mg^{2+}$, E_2–P_iMg^{2+}, and E_2Mg^{2+}·OUAB conformations, respectively, were all reduced less than 2% by the antibody. The antibody did, however, have an effect upon probe fluorescence in the presence of subsaturating concentrations of ligands. When subsaturating concentrations of K^+ (2 mM) were added to the E_1Na^+

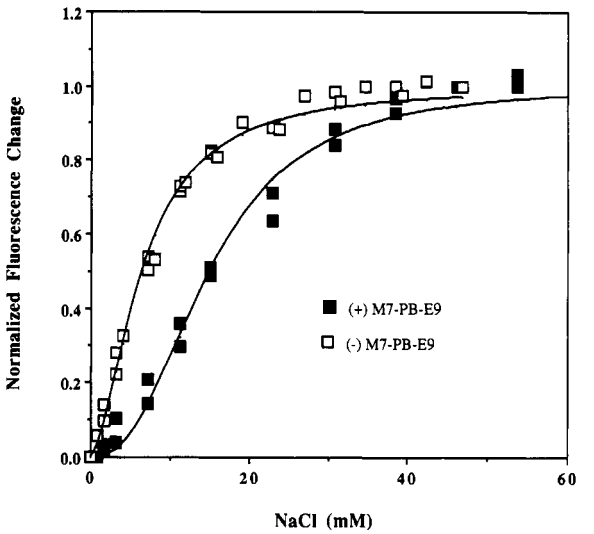

FIGURE 4: Effect of M7-PB-E9 on the Na^+-induced E_2 to E_1 conformational transition of Na^+,K^+-ATPase. FITC–Na^+,K^+-ATPase (2 μg/mL) in 2.4 mM KCl was titrated with NaCl (0–55 mM), and the Na^+-induced conformational change was monitored by FITC fluorescence intensity changes in the absence (open squares) and presence (closed squares) of 10 μg of M7-PB-E9. The antibody shifted the apparent K_d for Na^+ from 7 to 15 mM.

form of the enzyme, the antibody induced an 11% reduction in FITC fluorescence (data not shown).

The antibody effects on FITC–Na^+,K^+-ATPase fluorescence could then be explained if the antibody was shifting the poise of the equilibrium between the $E_1 \rightleftarrows E_2$ forms rather than directly altering a particular ligand's binding site. This was tested by titration of the FITC-labeled enzyme with various ligands in order to determine their binding affinities. In most cases, the ligand's apparent dissociation constant (K_d) was derived from the observed concentration-dependent fluorescence change. Figure 4 shows the relative change in fluorescence when the labeled enzyme, in 2.4 mM KCl (E_2K^+), was titrated with Na^+ ($E_2K^+ \rightarrow E_1Na^+$). The line drawn through the points is the best fit of the data to the Hill equation for cooperative binding. The presence of antibody had no effect on the extent of the response, but the apparent dissociation constant for Na^+ increased from 7 to 15 mM. The conformational transitions induced by K^+, Mg^{2+}, and P_i were measured in a similar manner, by monitoring the change in the steady-state fluorescence intensity. Ouabain, however, bound too slowly for convenient equilibrium measurements, and its binding was measured kinetically at a single concentration. As shown in Figure 5, ouabain binding to the enzyme, in the presence of 5 mM Mg^{2+}, caused a time-dependent fluorescence decrease that was adequately fit by a single-exponential binding equation (see Materials and Methods), and the antibody had a sizable 4-fold stimulatory effect which is in agreement with earlier work with [^{3}H]ouabain binding (Ball, 1984). Table II gives either the equilibrium dissociation constants or the second-order rate constants for the various ligand bindings tested.

The most obvious effect of the antibody was that it enhanced the binding of all ligands which caused an $E_1 \rightarrow E_2$ conformational change and inhibited the Na^+-dependent $E_2 \rightarrow E_1$ transition. This effect was clearly independent of the particular ligand used. For example, the K_d values for K^+ binding to the enzyme in 50 mM Tris buffer and in Tris plus 10 mM Na^+ were decreased (increase in affinity). Similarly, the K_d for phosphate binding to the enzyme with Mg^{2+} present decreased. Also, the rate of ouabain binding to the enzyme in both Mg^{2+} and $Mg^{2+}P_i$ conditions was stimulated.

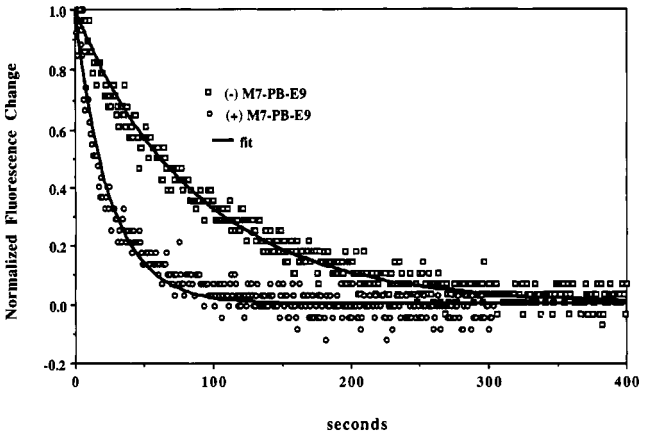

FIGURE 5: Effect of M7-PB-E9 on the ouabain-induced E_1 to E_2 conformational transition of Na^+,K^+-ATPase. FITC–Na^+,K^+-ATPase (4 μg/mL) in 10 mM $MgCl_2$ was mixed (mixing time 1 s) with 125 μM ouabain, and the ligand-induced conformational change (E_1 to E_2) was monitored by FITC fluorescence quenching (open squares). Preincubation of the enzyme with 10 μg of mAb M7-PB-E9 (open circles) increased the apparent rate of ouabain binding (see Table II). Rate constants were calculated from nonlinear least-squares fits to give first-order exponential decays of fluorescence (see Materials and Methods). The solid line curves show the calculated curve fit for each data set.

Table II shows that the antibody also affected ligand-induced transitions between different E_2 conformational states. For example, it increased the enzyme affinity for P_i when the $E_2K^+Mg^{2+}$ to E_2–$P_i(K^+)Mg^{2+}$ transition was induced, and it increased the rate of ouabain binding to the E_2–P_iMg^{2+} form of the enzyme. Interestingly, two conformational transitions were unaffected by the antibody. The Mg^{2+} affinity for the E_2K^+ conformation ($E_2K^+ \rightarrow E_1K^+Mg^{2+}$) was unaffected by the antibody, and the Na^+ affinity for the low-fluorescence E_2 (psuedo-E_2K^+ form) conformation induced by histidine buffer was not altered.

Effect of Enzyme Conformation on Antibody Affinity. Despite the fact that mAb M7-PB-E9 binds to the enzyme and specifically promotes ligand-caused conformational transitions to the E_2 forms and inhibits transitions to the E_1 forms, its binding seemed unaffected by the enzyme's conformation. The prior presence of either Na^+ or K^+ did not affect its ability to inhibit enzyme activity, and it appeared to bind to the E_1Na^+ conformation since it somewhat altered the fluorescence of the FITC-labeled enzyme. In order to more clearly determine whether enzyme conformation affected antibody affinity, the kinetics of antibody binding to the unlabeled holoenzyme in the E_1Na^+ and E_2K^+ conformations were measured by monitoring the light-scattering changes which occurred upon antibody binding. In this assay, antibody binding increases the average molecular weight of the enzyme–lipid vesicles, and the light-scattering intensity increases in proportion to the square of this relative mass increase (Nelsestuen & Lim, 1977), provided the wavelength of light (λ = 500 nm) is greater than the particle diameter [which was shown to be about 200 nm in diameter; see Van Winkle et al. (1976) and our unpublished observations]. Therefore, they should scatter light reasonably in proportion to their molecular weight squared (see Materials and Methods for details and electron microscopy results).

The upper tracing shown in Figure 6 shows the time dependence for the antibody-induced light-scattering enhancement. This tracing is the average of two experiments, and the overall error is shown by the signal to noise ratio. The maximal increase in light scattering was 15%. Figure 6 also shows the decrease in the fluorescence (11%) of FITC-labeled enzyme upon M7-PB-E9 binding with the enzyme in the mixed E_1Na^+/E_2K^+ conformation. Because the antibody concentration was approximately 3-fold higher (by weight) than that of the enzyme, the initial binding rates were approximately first order. The analysis of the time course of approach to maximum binding is shown in the Figure 6 inset as the log of the fraction of unbound sites remaining versus time. This semilog plot analysis is nonlinear in all three experiments, which is consistent with earlier on-rate measurements using an ELISA assay method (Ball, 1984). It is also apparent from these curves that the antibody binding rates under the three different ligand conditions and two different methods were identical for at least the first 70% of the binding process. Thus, with excess antibody, the binding shows little sensitivity to the E_1 or E_2 conformational state of the enzyme. The final 30% portions of the binding curves apparently diverged. However, this may be more apparent than real because the noise in the light-scattering signal is (about 8% of the total signal) amplified as the fraction of sites unbound nears zero.

DISCUSSION

Previous work showed that monoclonal antibody M7-PB-E9 inhibits Na^++K^+-dependent ATPase activity in competition with ATP and substitutes for ATP in stimulating the rate of ouabain binding (Ball, 1984). In the present study, bound antibody was found to facilitate or inhibit various ligand-caused enzyme conformational transitions rather than to have a direct effect at the ATP binding site. The antibody's apparent effect on ATP and other ligand affinities results from its alteration in the equilibrium between the $E_1 \rightleftarrows E_2$ forms of the enzyme. The bound antibody promotes a conformational change in the protein that includes the following series of intermediate conformations: $E_1 \rightarrow E_2K^+ \rightarrow E_2$–$P_iMg^{2+} \rightarrow E_2$–$P_iMg^{2+}$·ouabain.

Effect of Antibody on the ATP Binding Site. Although initial experiments suggested that the antibody could be binding at the ATP binding site, our current work using the ATP analogue eosin and the enzyme covalently labeled with FITC clearly indicated that this was not the case. For example, the antibody's affinity for the unlabeled enzyme (K_d = 3 nM) was unchanged by bound FITC. Also, the accessibility of FITC to solvent quenchers (I^-) and its orientational motions (anisotropy) were unaffected by bound antibody. The affinity and stoichiometry of eosin binding to the enzyme under high-affinity Na^+ conditions were also unaltered by the antibody. However, when subsaturating concentrations of K^+ were added to the E_1Na^+ form of the enzyme, the antibody decreased the affinity and the stoichiometry of eosin binding. These ligand conditions establish an equilibrium between the E_1Na^+ and the E_2K^+ conformations which have high (micromolar K_d) and low (millimolar K_d) affinities for ATP, respectively.

Effect of Antibody on Other Ligands. Our results indicate that M7-PB-E9 is an allosteric effector which does not directly affect any binding site of the enzyme. For example, it alters the binding of K^+ and ouabain, to their extracellular sites, while it binds to an intracellular site (Farley et al., 1986; Abbott and Ball, unpublished results). On the intracellular side of the membrane, ATP, Na^+, and P_i binding are all affected, but no ligand binding event was prevented by the bound antibody; instead, only the equilibria between different ligand states were shifted.

In general, the antibody's effects are explained by a shift of the $E_1 \leftrightarrow E_2$ enzyme conformational equilibrium to the right. This transition and its reversal are required for ion

Table II: Effect of mAb M7-PB-E9 on Conformational Transitions of FITC-Labeled Enzyme[a]

conformational transition	added ligand	equilibrium K_d, mM (n_H)		assocn rate constant (M^{-1} s^{-1})		% change in FITC fluorescence
		-mAb	+mAb	-mAb	+mAb	
E_1/Tris → E_2/Tris·K	K^+	0.077	0.032			-30
E_1Na → E_2K	K^+	6.2 (1.8)	4.3 (1.78)			-28
E_2K → E_1Na	Na^+	7.0 (1.8)	14.9 (2.0)			+28
MgE_1 → E_2–P_iMg	P_i	0.9 (1.2)	0.4 (1.2)			-28
MgE_2K → E_2–P_iKMg	P_i	5.97	2.33			-10
E_2/His → E_1/HisNa	Na^+	6.4	6.5			+20
E_2K^+ → MgE_2K	Mg^{2+}	0.33 and 16	0.24 and 14			+11
MgE_2P_i → E_2–P_iMg·OUAB	OUAB			220	320	-20
MgE_1 → E_2Mg·OUAB	OUAB			80	320	-50

[a] The intensity changes in FITC-labeled Na^+,K^+-ATPase fluorescence were used to monitor the binding of the physiological ligands and the inhibitor, ouabain, in the absence (-mAb) and presence (+mAb) of mAb M7-PB-E9. The normalized changes in fluorescence (see Figures 5 and 4) were fit to a single, independent-site binding isotherm where possible. The Hill equation was used for apparently cooperative binding (the Hill coefficient, n_H), and a two-site noncooperative binding model was used for the Mg^{2+} titration with the E_2K^+ → $E_2K^+Mg^{2+}$ transition. Also, the ouabain binding kinetics data, given as their second-order rates, were fit to a single-site pseudo-first-order binding model since the ouabain concentrations of 125 μM (Mg^{2+} conditions) and 50 μM ($Mg^{2+}P_i$ conditions) were saturating with respect to enzyme (≤12 nM).

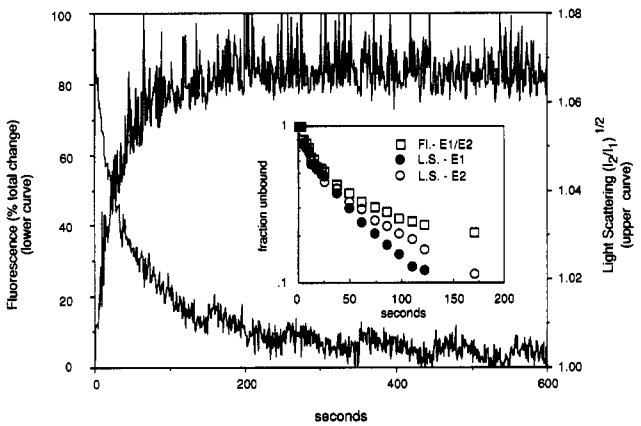

FIGURE 6: Determination of the effect of enzyme conformation on the mAb M7-PB-E9 binding rate. Antibody binding was initiated by adding 69 μg of antibody (180 nM final concentration) to 25 μg (80 nM) of Na^+,K^+-ATPase (or FITC-Na^+,K^+-ATPase) in 2.5 mL of buffer. The association rates with the enzyme in the E_1Na^+ (4 mM NaCl) conformation and the K^+ (0.2 mM KCl) E_2 forms were measured by light-scattering increases ($\lambda_{ex} = \lambda_{em}$ = 500 nm) and compared to the rate for an intermediate E_1/E_2 conformation (4 mM NaCl, 0.2 mM KCl) observed by the fluorescence decrease of the FITC-labeled enzyme. The upper curve shows the light-scattering increase in the presence of 0.2 mM KCl. The relative proteolipid molecular weight (M) increase is expressed in terms of scattering intensities: $\sqrt{I_{s2}/I_{s1}} = M_2/M_1$. The lower curve shows the decrease in FITC fluorescence intensity. The absolute light-scattering increase was 15%, and the fluorescence intensity decrease was 11%. Binding curves were normalized to 1, and the fractions of unbound sites versus time were plotted (inset, semilog plot) for the NaE_1 (closed circles, light-scattering E_1), the E_2K^+ (open circles, light-scattering E_2), and the Na^+/K^+ intermediate (open squares, FITC fluorescence, E/E_2) conformations.

transport and are the major conformational rearrangements observed in the enzyme. By monitoring FITC fluorescence, we found that the E_1 → E_2 or E_1 → E_2–P_i transitions induced by several ligands (K^+, Mg^{2+}+P_i, Mg^{2+}+ouabain, and $Mg^{2+}P_i$+ouabain) were each stimulated by the antibody while the Na^+-induced E_2 → E_1 was inhibited (see Table II). This result explains the antibody's effect on both eosin binding and enzyme activity. For example, the antibody inhibited eosin binding in the presence of nonsaturating K^+ concentrations because it enhanced the E_2 character induced by K^+. Also, the antibody's competitive inhibition with respect to ATP results from the decreased ability of ATP to induce the E_2 → E_1 conformational transition. Its stimulation of the ouabain binding rate is due to stimulation of the E_1Mg^{2+} + OUAB → E_2Mg^{2+}·OUAB transition.

In fact, the antibody appears to stabilize a sequence of ligand-induced changes. For example, it promotes the E_1-Na^+ to E_2K^+ transition and also promotes transitions from $E_2K^+Mg^{2+}$ to E_2–P_iMg^{2+} and from E_2–P_iMg^{2+} to E_2–P_i-Mg^{2+}·OUAB (see Table II). Apparently it lower the free energy (or ligand concentration) required for each of these transitions. This allows the ordering of these conformations according to their increasing, antibody-induced, stability: E_2–P_iMg^{2+}·OUAB > E_2–P_iMg^{2+} > E_2K^+ > E_1Na^+. This stepwise transition in the conformation includes a portion of the enzyme reaction cycle (plus the ouabain-induced dead-end inhibition step), and it nicely parallels the extent of observed FITC fluorescence decreases (Table II; Hegyvary & Jørgensen, 1981). Magnesium binding, however, was unaffected by the antibody.

In terms of the overall reaction cycle, M7-PB-E9 affects the K^+ transport half. This portion of the pathway, or K^+ ⇄ K^+ exchange, has been observed to operate in the absence of enzyme turnover. The tight binding or occlusion of K occurs in the absence of ligands with intracellular deocclusion in response to ATP and extracellular release in response to Mg·P_i in both red blood cells and reconstituted enzyme systems [see Glynn (1985) for a review]. The resulting conformational sequence for K^+ transport is E_1 ATP + K_{in} ↔ $E_2(K)$ ↔ E_2–P_i + K_{out}. These equilibria proceed to the left during the normal pump cycle, but they are shifted to the right by the antibody, thus inhibiting transport. The Na^+ transport portion of the cycle was not measured because ATP cannot bind to the FITC-labeled enzyme, but the overall E_1 ↔ E_2–P_i Mg^{2+} transition is accomplished by the cycle E_1 + ATP + Na_{in} ↔ E_1~P Mg^{2+}·ADP Na_{in} ↔ E_2–P Mg^{2+} Na_{out} ↔ E_2–P Mg^{2+}, and the antibody is expected to shift these equilibria to the right also.

The antibody should facilitate the E_1 → E_2 transitions by causing a very subtle change in enzyme structure, since the "in solution" rate of antibody binding with excess antibody is not noticeably affected by different ligands. In addition, bound antibody does not directly perturb the ATP binding pocket. Unlike antibody 9-A5 (Friedman & Ball, 1989) or mAb50s (Urayama et al., 1990), M7-PB-E9 does not cause, prevent, or limit the maximum extent of the ligand-induced effects. The epitope must be altered, however, by M7-PB-E9 in a manner which modifies the enzyme's response to ligand binding on both sides of the membrane. The important role that the epitope regions plays in the E_1 ↔ E_2 transitions makes the identification of its sequence location the subject of ongoing work. Further, it will be interesting to determine whether there are strict amino acid sequence requirements in order for

this region to function properly. At this time, we have shown that M7-PB-E9 recognizes all mammalian, digitalis-sensitive enzymes that we have tested but not rat α_1 which is highly insensitive nor rat α_2 which has an intermediate sensitivity to inhibition by digitalis. How the sequence alterations that occur in the epitope may affect the $E_1 \rightarrow E_2$ transitions, or at least the cardiac glycoside-dependent ones, remains to be determined.

ACKNOWLEDGMENT

We thank Dr. Donald Ferguson of the University of Cincinnati for the electron microscopy work.

REFERENCES

Abbott, A. J., Amler, E., & Ball, W. J. (1991) *Biochemistry 30*, 1692–1701.
Ball, W. J. (1984) *Biochemistry 23*, 2275–2281.
Ball, W. J. (1986) *Biochemistry 25*, 7155–7162.
Doty, P., & Edsall, J. T. (1951) *Adv. Protein Chem. 6*, 35–121.
Farley, R. A., Ochoa, G. T., & Kudrow, A. (1986) *Am. J. Physiol. 250*, C896–C906.
Friedman, M. L., & Ball, W. J. (1989) *Biochim. Biophys. Acta 995*, 42–53.
Geering, K. (1991) *FEBS Lett. 285*, 189–193.
Glynn, I. M. (1970) *J. Physiol. 207*, 371–391.
Glynn, I. M. (1985) in *The Enzymes of Biological Membranes* (Martonosi, A. N., Ed.) Vol. 3, pp 35–114, Plenum Press, New York.
Glynn, I. M., Hoffman, J. F., & Lew, V. L. (1971) *Philos. Trans. R. Soc. London B262*, 91–102.
Hegyvary, C., & Jørgensen, P. L. (1981) *J. Biol. Chem. 256*, 6296–6303.
Karlish, S. J. D., Goldschleger, R., & Stein, W. D. (1990) *Proc. Natl. Acad. Sci. U.S.A. 87*, 4566–4570.
Lane, L. K., Potter, J. D., & Collins, J. H. (1979) *Prep. Biochem. 9*, 157–170.
Lowry, O. H., Rosebrough, N. J., Farr, A. L., & Randall, R. J. (1951) *J. Biol. Chem. 193*, 2165–2175.
Moczydlowski, E. G., & Fortes, P. A. G. (1981) *J. Biol. Chem. 256*, 2346–2356.
Nelsestuen, G. L., & Lim, T. K. (1977) *Biochemistry 16*, 4164–4177.
Pedemonte, C. H., & Kaplan, J. H. (1990) *Am. J. Physiol. 258*, C1–C23.
Price, E. M., & Lingrel, J. B. (1988) *Biochemistry 27*, 8400–8408.
Schwartz, A., Allen, J. C., & Harigaya (1969) *J. Pharmacol. Exp. Ther. 168*, 31–41.
Silverton, E. W., Navia, M. A., & Davies, D. R. (1977) *Proc. Natl. Acad. Sci. U.S.A. 74*, 5140–5144.
Skou, J. C., & Esmann, M. (1981) *Biochim. Biophys. Acta 647*, 232–240.
Taylor, W. R., & Green, N. M. (1989) *Eur. J. Biochem. 179*, 241–248.
Urayama, O., Nagamune, H., Nakao, M., & Hara, Y. (1990) *Biochim. Biophys. Acta 1040*, 207–275.
Van Winkle, W. B., Lane, L. K., & Schwartz, A. (1976) *Exp. Cell Res. 100*, 291–296.